LFMCW based MIMO imaging processing with Keystone Transform

Philip van Dorp
Radar department
TNO
The Hague, The Netherlands
philip.vandorp@tno.nl

***Abstract*—In this paper, a new signal processing technique for Multiple-Input Multiple-Output (MIMO) image processing of a Linear Frequency-Modulated Continuous Wave (LFMCW) automotive radar was developed. The image is the range-speed-direction data cube. The technique comprises two improvements to the standard MIMO image processing: 1) A fast unambiguous Doppler target detection. 2) An improved direction finding with estimated virtual antenna elements besides the synthesized virtual antenna elements. High speed automotive targets go through several range cells in the observation period making it difficult to obtain coherent accumulated power. Another problem with high speed targets in combination with a low Sweep Repetition Frequency (SRF) is ambiguous Doppler speed measurement. In order to remove range migration and obtain coherent accumulated power the keystone transform is applied. The direction finding resolution depends on the number of transmitter- and the receiver elements of the MIMO configuration. A combination of the transmitter and receiver elements give synthesized virtual elements with corresponding antenna width. In order to improve the direction finding, the antenna width with extrapolated virtual antenna elements was extended. The Band Width Extrapolation (BWE) method is applied for estimating these extrapolated virtual antenna elements. The proposed method is verified by simulation and real radar measurements.**

Keywords — MIMO radar; Keystone transform, Band Width Extrapolation; Automotive radar; Unambiguous Doppler speed estimation.

I. INTRODUCTION

The mechanism of phased array radar is well known. The combination of phased array with the MIMO concept and LFMCW waveform resulted in reduced costs, -power consumption, -weight, -size, -hardware and -software complexity and processing time, as well as improved direction finding; all can be achieved simultaneously. For these reasons MIMO phased array radars with LFMCW waveform are attractive in automotive applications.

However, there are some disadvantages to be solved. (1) The long coherent observation time required for an accurate measurement and MIMO beam forming. This time is in conflict with the required fast accurate high-speed target detection for automotive applications where targets migrate in range. The range migration results in a non-coherent accumulated power in the range-speed-direction data cube. (2) The ambiguous Doppler speed caused by the low update rate of one MIMO beam forming cycle. (3) The size of the antenna. A larger antenna array aperture produces a more robust angle resolution and more accurate angle estimation for closely spaced targets. The antenna size is limited for most applications e.g. automotive radars.

In this paper two improvements of the standard MIMO processing are described. The first improvement is the Keystone transform, see [1], to remove the range migration, obtain coherent accumulated power and to be solve the unambiguous Doppler speed estimation. The second improvement is direction finding with estimated virtual antenna elements besides the existing synthesized virtual antenna elements. These extra elements improve the resolution angle to obtain a better target separation and more accurate direction. Van Dorp [2] describes that the order of succeeding processing steps with BWE gives different sensitivity to noise or artifacts. The correct processing order to obtain the range-speed-direction data cube with direction BWE is (1) range processing, (2) speed processing and (3) direction processing.

The remainder of this paper is organized as follows: in section II the theory is formulated; it starts with a general overview of the processing, followed by the Keystone transform, improved direction finding and MIMO processing. Section III presents simulations of the method and results of real radar measurements. Finally the conclusions are presented in section IV.

II. THEORY

LFMCW based MIMO processing is described in [3], [4] and [5]. If N_T transmitter elements and N_R receiver elements are positioned in a suitable manner, an equidistant array of $N_T N_R$ virtual elements can be synthesized with only $N_T + N_R$ elements. MIMO processing assumes that independent signals for each transmitter-receiver combination are available. In order to synthesize the total number of $N_T N_R$ MIMO channels, transmitter time division is applied. The transmitter signals are switched on or off for transmitting only one transmitter in the sequence $1,2,\cdots,N_T$. The sweep repetition time is T. One sequence gives measurements for one range-direction response. In order to estimate the Doppler speed, N_S sequences are transmitted. However the effective SRF is reduced by the number of transmitters $SRF_e = 1/(N_T T)$ and reduces the unambiguous Doppler speed.

Fig. 1 represents the following processing architecture: Keystone transform part 1 interpolation, part 2 phase ambiguity compensation, range-speed processing, virtual element extrapolation, MIMO beam steering, detection, plot extraction and combined plots. The phase ambiguity compensation, explained in subsection IIA, provides maximum coherent accumulated power if the folding factor l is equivalent with the measured target Doppler folding. In case of no match there is incoherent accumulated power. Selection of the maximum accumulated power results in the folding factor and corresponding unambiguous speed. Since the target speed is unknown, the architecture splits into parallel processes with different folding factors. Fig. 1 represents the principle three parallel processes with $l = -1,0,+1$.

The radar measurement cube enters the architecture in the top and represents the measurements data. The cube has three dimensions: (1) The fast time t is the time in which the received LFMCW signal digitized with sample frequency f_s and sweep length is T_0. (2) The slow time on one transmitter is the sweep counter n_S and N_S sweeps are transmitted for each transmitter. (3) The $N_T N_R$ MIMO virtual elements. The range-speed-direction data cube gives the result after MIMO beam steering processing.

Combine plots compares the incoherent and coherent accumulated power of the three range-speed-direction data cubes and select the best folding factor resulting and hence the best unambiguous speed.

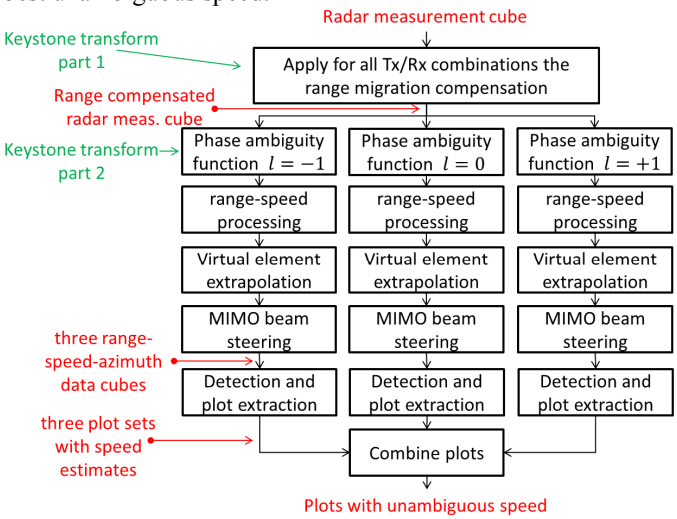

Fig. 1. Processing scheme of the LFMCW based MIMO processing.

A. Keystone Transform

The Keystone transform comprises two parts: (1) A range migration compensation by interpolation of the LFMCW measurements. (2) Ambiguous speed compensation by multiplication with a phase ambiguity function, see [1].

Part (1): The n_Sth LFMCW return signal on one of the N_R receivers can be written as:

$$s(t,n_S) = a\left(t - 2\frac{R_0+vn_ST}{c}\right)\exp\left(-j2\pi f_c\frac{2(R_0+vn_ST)}{c}\right)$$
$$\exp\left(j2\pi f_d t\right) \quad (1)$$

where

$$a(t) = rect(\frac{t}{T_0})\exp\left(j\pi\gamma t^2\right) \quad (2)$$

here, R_0 is the target initial position; v is the target radial velocity; f_d is the target Doppler frequency; γ the frequency modulated slope. The frequency modulated slope is $\gamma = B/T_0$ where B is the sweep bandwidth. The Fourier transform of the return signal over the fast-time variable gives the range response. The phase component $\varphi(t)$ of the range response gives the coupling between f and v which indicates a range migration:

$$\varphi(t) = -2\pi(f+f_c)\frac{2vn_ST}{c} - 2\pi(f+f_c)\frac{2R_0}{c}. \quad (3)$$

The Keystone transform compensates the range migration and is a linear coordinate expressed as $n_S = (f_c n_S^K)/(f_c+f)$. Substitution of n_S removes the coupling between f and v:

$$\varphi(t) = -2\pi f_c\frac{2vn_S^KT}{c} - 2\pi(f+f_c)\frac{2R_0}{c}. \quad (4)$$

The coordinate transformation n_S to n_S^K is a time interpolation of the LFMCW return signal in two steps. (a) The FFT resampling is applied with a high resampling factor, e.g. 16, and preserves the spectral content. (b) A piecewise linear interpolation is applied between two adjacent points.

Part (2): When the target radial speed is high and the radar has low SRF, under-sampling will occur and gives ambiguous speed measurements. This under-sampling can be compensated by multiplication with a phase ambiguity function. The phase ambiguity function depends on the time to perform one complete MIMO range-direction response and is expressed in following equation:

$$H = \exp\left(-j2\pi lSRF_e\frac{f_c}{f_c+f}n_S^K\right), \quad (5)$$

where l is the folding factor and SRF_e is the effective SRF. The folding factor gives the number of SRF_e's. If the target speed is ambiguous, the folding factor gives the unambiguous speed.

B. Range-Speed Transform

The range-speed transform is applied for all transmitter-receiver combinations. The resulting range-speed responses are $U_{nm}(r,v)$ with transmitter counter n and receiver counter m. The range-speed transform is performed with a two dimensional Fast Fourier Transform and windowing function in both directions. The range-speed responses are time aligned for time division with a frequency shift which depends on the Doppler frequency and the transmitter counter n:

$$b_n(v) = \exp\left(-j2\pi\frac{2vf_c}{c}(n-1)T\right) \quad (6)$$

C. Virtual Element Extrapolation

The coherent MIMO phased array radar consists of separated transmitter and receiver elements. The placement of the transmitter and receiver elements gives an Uniform Linear Array (ULA) of synthesized virtual elements. An example of this is presented in Fig. 2, see [5].

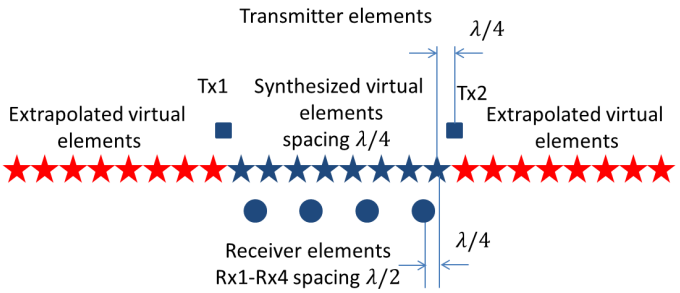

Fig. 2. Illustration of an 8-element MIMO radar topology.

The extrapolated virtual elements are estimated with direction BWE, see [6], [7] and [2]. The previous processing step gives the range-speed-direction data cube without the direction processing. The data cube contains $N_T N_R$ range-speed responses, one for each synthesized virtual element. Each range-speed cell has a vector of $N_T N_R$ elements with all direction information. BWE is applied individually onto each vector and predict additional virtual elements on both sides of the synthesized ULA. After extrapolation the range-speed-direction data cube has N_P range-speed responses: the synthesized responses and the extrapolated responses. The extrapolation factor is $N_E = N_P/(N_T N_R)$.

D. MIMO Phased Array Radar

Assume x_n^{Tx}, $n = 1, \cdots, N_T$ are the positions of the transmitter phase centers and x_m^{Rx}, $m = 1, \cdots, N_R$ are the positions of the receiver phase centers. The 3D coordinate of the target is z. The travelling way to the target and back is given by $R_{nm}(z) = R_n^{Tx}(z) + R_m^{Rx}(z)$ with $R_n^{Tx}(z) = |z - x_n^{Tx}|$ and $R_m^{Rx}(z) = |z - x_m^{Rx}|$. If the far-field condition is fulfilled, the synthesized and extrapolated virtual elements can be approximated by $x_{nm} = \frac{1}{2}(x_n^{Tx} + x_m^{Rx})$ as part of $R_{nm}(z) \approx 2|z - x_{nm}|$. x_{nm} is the virtual phase center of the transmitter and receiver and indicates the synthesized and extrapolated virtual elements. x_{nm} synthesizes the ULA and can be calculated for synthesized virtual elements and extrapolated virtual elements. In x_{nm}, nm changes from $nm \to p$, with $p = 1, \cdots, N_P$ and subsequently x_p denotes the phase center. p counts all virtual phase centers. The corresponding MIMO steering vector is

$$a_p = \exp\left(-j4\pi \frac{x_p \sin(\theta)}{\lambda}\right) \tag{7}$$

where λ is the wavelength and θ the steering angle. For a given range r and speed v the direction can be calculated with:

$$P(r, v, \theta) = \sum_{p=1}^{N_P} U_p(r, v) w(\theta) a_p(\theta) \tag{8}$$

where $w(\theta)$ is an angle window function. $P(r, v, \theta)$ is the range-speed-direction data cube.

III. Results

Two experiments are carried out applying the described method. The first experiment contains simulated targets with typical automotive radar settings. The second experiment contains real measurements of a MIMO surveillance radar.

A. Simulated Automotive Radar

The simulated system MIMO topology is presented in Fig 2. The system specifications are $f_c = 77$ GHz, $B = 1$ GHz, $T = 50$ µs, $T_0 = 45$ µs, $f_s = 10$ MHz , $N_T = 2$, $N_R = 2$, $N_E = 3$ and $N_S = 256$. Hamming window functions are applied. The unambiguous Doppler speed is $v_{max} = 9.74$ m/s. The response is calculated on a range-speed-azimuth grid with range grid size Δr= 0.15 m, Doppler speed grid size $\Delta v =$ 0.15 m/s, angle grid size $\Delta\theta$ = 1º, and three folding factors $l = -1, 0, +1$.

Fig. 3 presents the results in the range-azimuth plane. The maximum Doppler amplitude is selected $P(r, \theta) = max_v(P(r, v, \theta))$. The simulated target amplitudes have 1 V ADC amplitude, the added noise is 30 dB. Four different target categories are simulated with increasing range, see Fig. 3:

Category 1: Seven slow moving targets with -9, -6, -3, 0, 3, 6, 9 m/s unambiguous radial speed and absolute cross-range speed smaller than 2 m/s.

Category 2: Ten targets with equivalent range, 2º, 4º, 6º, 8º, 10º, 12º, 14º azimuth spacing and -9 m/s radial speed.

Category 3: Six fast speed targets with equivalent range, ±19.5 m/s radial speed ($\approx 2v_{max}$) and ±29.0 m/s radial speed ($\approx 3v_{max}$) but different azimut angle.

Category 4: Five targets with -19.5 m/s radial speed and 5, 10,15, 20, 25 m/s cross-range speed.

The results per category are as follows:

Category 1: The targets gives maximum coherent accumulated power on the correct position and correct Doppler speed. The average target power is 65.0 dB with $l = 0$, corresponding to no unambiguous radial Doppler speed. The targets have 58 dB accumulated power for $l = -1$ and $l = +1$. The Keystone transform suppression is 7 dB.

Category 2: Targets at $l = 0$, with azimuth spacing smaller than 10º cannot be individually distinguished. The effective angular resolution, if two peaks are to be resolved, is $\Delta\theta_e = \lambda W_{6dB}/(2A_e) = 9º$ where W_{6dB} is the angle window correction factor and A_e the effective aperture length of the virtual array, see [5] and [8]. The estimated angular resolution is close to the theoretical value.

Category 3: All targets give maximum signal power if the folding factor corresponds with the unfolded Doppler speed. The average power is 66 dB for ±19.5 m/s Doppler speed and 65 dB for ±29.0 m/s Doppler speed. There is a degradation in the coherent summation in case of fast targets. The signal power of the unfolded incorrect solution has 2 dB lower signal power and the blurred solution 7 dB lower signal power.

Category 4: The targets have a correct position and folding factor. The average power with correct folding is 65.5 dB, the folded incorrect solution 64 dB, and the blurred solution 59 dB.

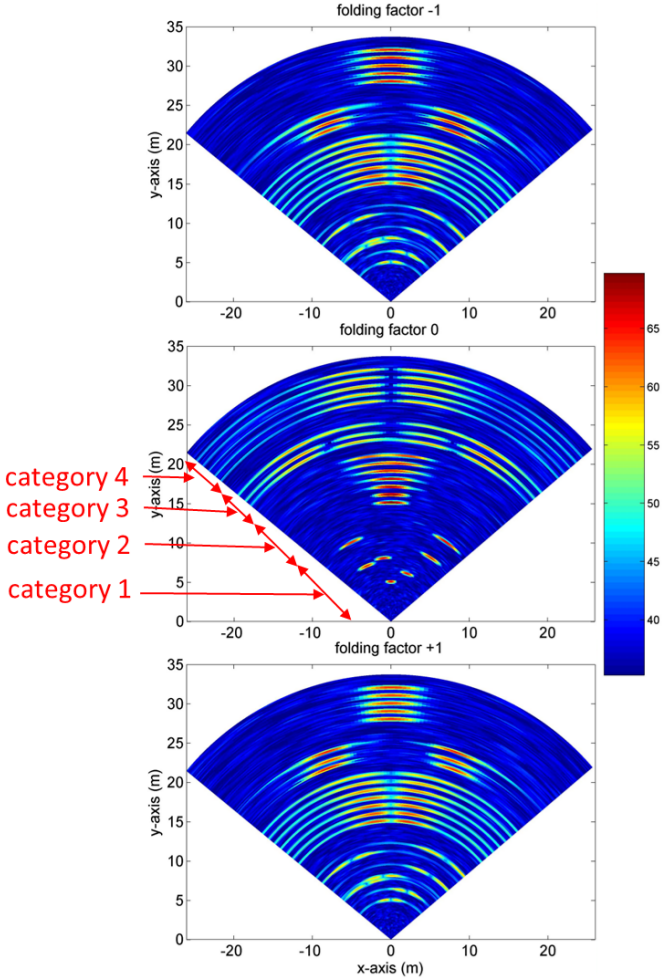

Fig. 3. Simulated automotive radar range-azimuth results for three folding factors. The four target categories are indicated.

B. MIMO Surveillance Radar

A demonstration system for coherent MIMO radar has been developed by TNO for surveillance applications. The MIMO configuration is described by Huang [5]. The system specifications are $f_c = 13.7$ GHz, $B = 150$ MHz, $T = 50$ µs, $T_0 = 45$ µs, $f_s = 10$ MHz , $N_T = 4$, $N_R = 4$, $N_E = 3$ and $N_S = 256$. The synthesized virtual array length is 10, overlapping virtual elements are ignored. Hamming window functions are applied. The unambiguous Doppler speed is $v_{max} = 9.74$ m/s. A number of experiments were performed with walking human, running human and cyclists. Fig. 4 presents a view of the scenario- and the range-azimuth results of a walking human and cyclist. The results correspond with the theory. The cyclist's radial speed is ambiguous and estimated unambiguously.

IV. CONCLUSIONS

In this paper, a new signal processing technique for Multiple-Input Multiple-Output (MIMO) image processing of a Linear Frequency-Modulated Continuous Wave (LFMCW) automotive radar is presented. The technique combines the Keystone transform and improved direction finding with virtual antenna element extrapolation. The results show that the Keystone interpolation gives correct range migration compensation. The phase ambiguity function provide maximum coherent accumulated power if the folding factor is equivalent with the measured Doppler speed folding, otherwise there is incoherent accumulated power. Virtual antenna element extrapolation gives a smaller angular resolution.

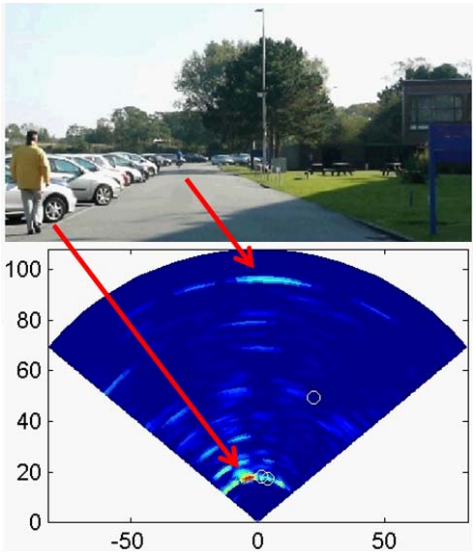

Fig. 4. MIMO surveillance radar measurements with walking human and cyclist. Zero Doppler speed targets are suppressed.

ACKNOWLEDGMENT

The author thanks A.J.M. de Graauw and C. Gehrels of NXP Semiconductors for their support.

REFERENCES

[1] R. Perry, R. DiPietro and R. Fante, "Coherent Integration With Range Migration Using Keystone Formatting," *MITRE,* 2007.

[2] P. v. Dorp, R. Ebeling and A. Huizing, "High resolution radar imaging using coherent multiband processing techniques," *IEEE Radar Conference 2010,* pp. pp. 981-986, 2010.

[3] J. Li and P. Stoica, MIMO Radar Signal Processing, John Wiley and Sons, 2009.

[4] J. Ender and J. Klare, "System architectures and algorithms for radar imaging by MIMO-SAR," *IEEE Radar Conference 2009,* 2009.

[5] Y. Huang and P. Brennan, "FMCW Based MIMO Imaging Radar for Maritime Navigation," *Progress In Electromagnetics Research,* vol. Volume 115, pp. pp. 327-342, 2011.

[6] I. Kauppinen and K. Roth, "Audio Signal Extrapolation - Theory and Applications," *International Conference on Digital Audio Effects (DAFx-02),* pp. pp. 105-110, 2002.

[7] K. Roth, I. Kauppinen, P. Esquef and V. Valimaki, "Frequency Warped Burgs Method for AR-Modelling," *IEEE Workshop on Applications of Signal Processing to Audio and Acoustics,* October 19-22 2003.

[8] F. Harris, "On the Use of Windows for Harmonic Ananysis with the Discrete Fourier Transform," *Proceedings of the IEEE,* vol. Vol. 66, no. No. 1, 1978.